Linear viscoelasticity of wormlike micelles: a comparison of micellar reaction kinetics

M. Turner, M. Cates

Classification
Physics Abstracts
36.20 — 82.30 — 62.10

Linear viscoelasticity of wormlike micelles: a comparison of micellar reaction kinetics

M. S. Turner and M. E. Cates

Cavendish Laboratory, Madingley Road, Cambridge CB3 0HE, G.B.

(Received 26 August 1991, accepted 15 November 1991)

Abstract. — Stress relaxation in worm-like micelles and other "living polymers" is governed by an interplay between simple reptation and intermicelle reactions. A simple model of stress relaxation is used in which the linear viscoelastic functions can be written as averages over a certain one-dimensional stochastic process. A detailed numerical study was recently made for the case when scission and end to end recombination reactions are present (Turner M. S. and Cates M. E., *Langmuir* **7** (1991) 1590). In the present work we use the same approach to study other reaction mechanisms. We consider both end-interchange, where the end of one chain "bites" into the sequence of another, and bond-interchange, where chains exchange material by formation of a fourfold-coordinated intermediate. We find that end-interchange results in quantitatively similar viscoelastic behaviour to the reversible scission case: for $\tau_{\rm break} \lesssim \tau_{\rm rep}$ the terminal time τ is much reduced from the reptation value and the spectrum becomes monoexponential with $\tau \sim \tau_{\rm break}^{1/2}\tau_{\rm rep}^{1/2}$. Here $\tau_{\rm rep}$ is the reptation time of a hypothetical unbreakable chain of the average length, and $\tau_{\rm break}$ a suitably defined micellar scission time. For the case of bond-interchange we predict qualitatively similar behaviour, although the terminal time τ is less strongly affected than for the other two reaction schemes; in the regime $\tau_{\rm break} \ll \tau_{\rm rep}$ we predict $\tau \sim \tau_{\rm break}^{1/3}\tau_{\rm rep}^{2/3}$. This result is also confirmed in the numerical study. Finally we include an idealised treatment of constraint release which suggests that the effect of tube renewal on stress relaxation is relatively weak in these systems. We use the Cole-Cole representation of the frequency-dependent modulus $G^*(\omega)$, which provides a sensitive method of probing the relaxation. Comparison of our calculated plots with experimental viscoelastic data may provide, in principle, a method for determining the reaction mechanisms present in any given system.

1. Introduction.

"Living polymers" are polymers, or other chainlike objects, which can exchange material by reversible reactions. Living polymers are thought to exist in aqueous systems such as CTAB/KBr and CTAC/NaSal [1-13] which, under appropriate conditions, are known to assemble reversibly into flexible worm-like micelles [14]. These are, in favourable cases, extremely long (many thousand Ångstroms), flexible and undergo reactions on a relatively rapid time scale. In the simplest case these reactions consist of a forward (scission) reaction where the micelle spontaneously

breaks at a random point along its length, and the reverse (recombination) reaction where one micelle combines end-to-end with another. The dynamics of entangled polymers, which can undergo reversible scission reactions, has received recent theoretical attention [14-19]. It has been found that, at least in certain systems, such as CTAB/KBr, a model [15-17] including only end-to-end reactions can accurately describe the dynamics for both stress relaxation [14] and relaxation following temperature jump [13,18] in a consistent way. However it was recognised from the outset [15-17] that end-to-end reactions are not the only reactions possible, and in several other systems, such as CTAC/NaSal+NaCl, there is good evidence [20] to suggest that the dominant reactions are different.

Several recent experiments [2-5] concern the frequency dependent linear shear modulus $G^*(\omega)$ for these systems which can be presented in the form of a Cole-Cole plot, in which the imaginary part of the complex modulus (the loss modulus G'') is plotted against the real part (the storage modulus G'). This proves to be a highly sensitive method of probing the precise form of $G(t)$ [19] and we will use it in the present work.

The original theoretical model of references [15-17], described in more detail below, predicts single exponential stress relaxation and hence a semi-circular Cole-Cole plot, in the regime where end-to-end scission/recombination reactions are rapid on the time scale of reptation [21] of an average chain. We shall find that this prediction, which is well confirmed in experiments on several types of wormlike micellar system [2-5], is also consistent with other forms of reaction kinetics (described in Sect. 2). In the present work, we give a detailed numerical analysis of the model over a wide range of reaction rates and, for the first time, we include different reaction kinetics. We also include a treatment of constraint release in order to model the effect of tube renewal on stress relaxation.

An experimental method, known as Temperature jump (T-jump), can be used to measure the timescale on which individual wormlike micelles undergo simple scission reactions [18]. The present work provides a quantitative description of the effects of various types of reaction kinetics and can be compared directly with experimental viscoelastic data. Hence, in systems where both viscoelastic and T-jump data are available, it may now be possible, in principle, to determine which reaction mechanism dominates.

2. Model for reaction kinetics.

In the entangled regime, each polymer (micelle) is constrained by a "tube" (consisting of the entanglements of the polymer with its neighbours) [22]. We consider first the imposition of a small step strain on the system, which is taken to be at equilibrium initially. The effect of this small strain is to constrain the polymer to a non-equilibrium conformation. The stress associated with this is relaxed by curvilinear diffusion (reptation) of the chain out of its initial tube and into a new tube, which is at equilibrium. In the absence of any interchain reactions this process is well understood [21]. However the dynamics of stress relaxation are complicated by the processes of the chain reactions. We first introduce the various reaction mechanisms which we consider here.

(i) *Reversible scission.* This reaction scheme consists of a forward, unimolecular scission reaction and a reverse, bimolecular recombination rection. The scission reaction is characterized by a rate constant k_s per unit time per unit arc length and is assumed to be independent of polymer length. By detailed balance the recombination reaction must therefore proceed by two chains fusing end-to-end (Fig. 1). Recombination is characterized by a second rate constant k_s' per unit time and the overall rate is proportional to the square of the concentration of chain ends.

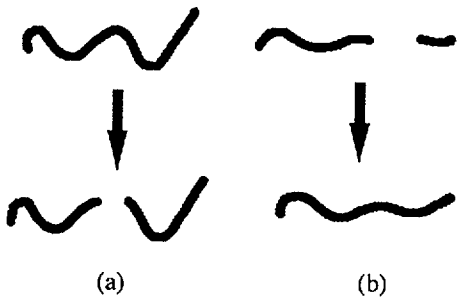

Fig. 1. — A diagram representing the time evolution of, (a) a scission process, and (b) a recombination process.

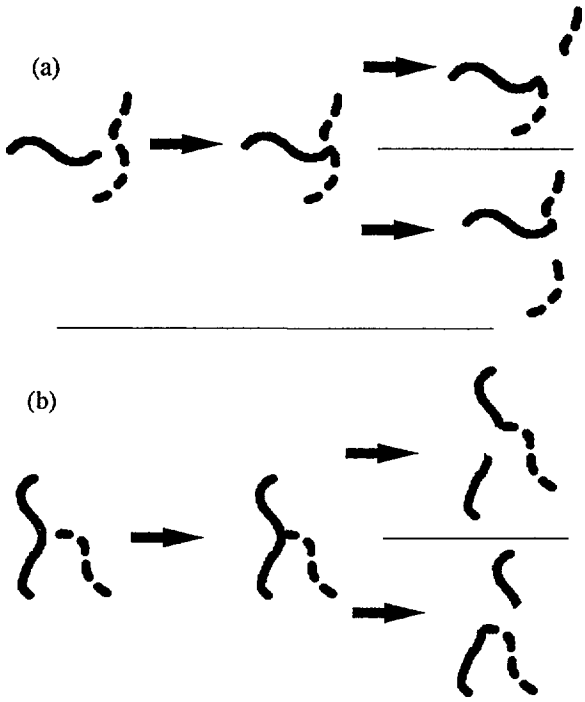

Fig. 2. — A schematic plot of the time evolution of, (a) an A-type end-interchange process, and (b) a B-type end-interchange process.

(ii) *end-interchange reactions.* end-interchange reactions occur when the end of one chain "bites into" a second chain at a random position along its length. A transient structure resembling a three-armed star polymer is formed briefly, which decays to give two new chains, the end of the first chain having fused to a section of the second chain, chosen at random, the other section breaking off (Fig. 2). This process is characterised by a rate constant k_e and the overall rate is proportional both to the arc length concentration and the concentration of

chain ends. We have defined this reaction so as not to include the case when the two segments of the second chain recombine with each other, giving no net change in the length of either chain. (This is likely to happen in practice of course but merely amounts to a trivial rescaling of the rate constant.)

(iii) *bond-interchange reactions.* bond-interchange reactions are reactions whereby two chains come into contact and react at some point along their arc lengths, chosen at random. A transient structure resembling a four-armed star polymer is formed briefly, decaying to give two new chains with each section of the first chain fusing to one or other section of the second chain, chosen at random (Fig. 3). This reaction is characterised by a rate constant k_b and the overall rate is proportional to the square of the arc length concentration. As in the case of end-interchange in defining k_b we exclude reactions whereby the transient state decays back into its original components.

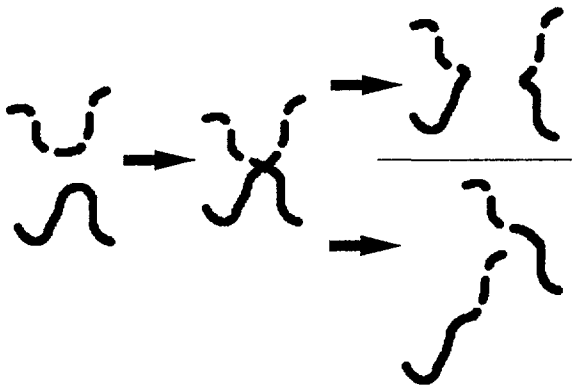

Fig. 3. — A diagram representing the time evolution of a bond-interchange process.

In what follows we adopt a mean field approach which assumes all reactions are uncorrelated in time. This assumption should be valid for flexible chains at moderately high concentration [14].

We assume that the local reaction rate constants, k_s, k_s', k_e and k_b, do not depend on chain length. This assumption is appropriate in the entangled regime when reaction rates are determined by the local motion of subsections of chain, and not the diffusion of polymers over distances large compared to their gyration radii. Even in the dilute regime, where it may be possible to include approximate expressions for the chain length dependence of the rate constants, corrections to the mean field approach also become necessary and so we ignore the effect for simplicity.

Factors such as as the precise chemical components, salinity and temperature will determine which of the three reaction mechanisms detailed above are present. On a microscopic scale we expect the attempt frequency for bond-interchange to be very much greater than the attempt frequency for end-interchange which in turn will be very much greater than the attempt frequency for recombination. However each of the three reaction schemes will also have a different activation energy with the bond and end-interchange reactions typically having a much higher activation energy than simple scission.

Note that bond-interchange reactions allow one chain to cross through another via the four-armed intermediate state. This implies that chain entanglements may not always be effective

in constraining the lateral motion of the polymer. However it can be shown [23] that the tube model remains valid, even when chain reactions are rapid on the timescale of reptation (one only requires that the micelle reactions occur on a timescale which is much larger than the Rouse time of the average chain). This allows a large regime where such reactions can be detected in the shape of the stress relaxation function without a total breakdown of the reptation description.

The present model does not include reactions involving more than two chains, which we expect to be rare, nor does it include micellar rings the effect of which on stress relaxation might be expected to be small, especially in concentrated systems [14]. For the same reason we must exclude intra-chain reactions which necessarily result in ring formation.

3. Stress relaxation.

The motion of a chain in a concentrated environment of other chains is well understood in terms of the reptation model [21]. This model describes the spatial constraints imposed by the neighbouring chains in terms of a "tube" in which the chain resides. This tube limits the lateral movement of the chain but allows curvilinear diffusion in much the same way as a snake moves through tall grass. The stress relaxation mechanism model of references [15-17] can be modified to include end- and bond-interchange reactions and can be cast as a one-dimensional stochastic process in the following way. The curvilinear diffusion constant of a chain in its tube $D_c(L)$ varies as L^{-1} Since stress is associated with the deformation of tube segments, it is easier to imagine the chain stationary and the tube diffusing relative to it. In this case, a given tube segment relaxes when it reaches the end of the chain. The motion is that of a hypothetical "particle" (representing a tube segment) of diffusivity $D_c(L)$ on a line of length L (representing the chain) with absorbing boundary conditions at the chain ends.

We may include the effects of the chain reactions by allowing the absorbing ends of the line segment to make random jumps with appropriate transition probabilities. These are defined in section 3.1 for the three different reaction schemes. By averaging over all starting positions of the particle on the line (equivalent to averaging over all tube segments), and all initial chain lengths, one obtains the survival probability of the particle to time t, which is the fraction of original (stressed) tube through which no chain end has passed up to that time, written $\mu(t)$. (Clearly $\mu(0) = 1$ and $\mu(t) \to 0$ as $t \to \infty$.) The probability distribution for the initial chain length is determined by the fact that, in accordance with the predictions of equilibrium statistical mechanics [14], the steady state chain length distribution is exponential with mean $\bar{L} \sim (k_s'/2k_s)^{1/2}$

A problem with this description is that the tube will in fact be "evolving" as the constraints making up the tube reptate away. This effect may become important in systems that are close to the overlap threshold rather than strongly entangled. We discuss this effect further in section 4, but will ignore it in the remainder of section 3.

In linear viscoelasticity one measures properties such as $G^*(\omega)$ which are related through integral transforms to the stress relaxation function $G(t)$. We can define $G(t)$ in terms of $\mu(t)$ as

$$G(t) \equiv G_o\, \mu(t) \tag{1}$$

Where G_o is called the plateau modulus (the stress imposed per unit strain at $t = 0$).

3.1 NUMERICAL STUDY. — A suitable numerical algorithm already exists [15,19] for the calculation of $\mu(t)$ when *only* reversible scission reactions are present. This algorithm has

already been implemented with the necessary precision [19] and a transform into the frequency domain has been carried out. Here we extend the model to include our two new reaction schemes and, in section 4, a preliminary treatment of tube renewal effects. For each reaction scheme we compute $\mu(t)$ for various values of a parameter ζ which governs the frequency of chain reactions. This parameter obeys $\zeta = \tau_{\text{break}}/\tau_{\text{rep}}$, where τ_{rep} is the reptation time of a chain of the average length $\bar{L}$ and τ_{break} is a characteristic time for reaction processes. This is defined seperately for each reaction scheme in sections 3.2, 3.3 and 3.4.

The program starts with a particle on a line whose left and right segments (L_{left} and L_{right} respectively) are chosen independently from an exponential distribution of unit mean. (Thus we choose units so $\bar{L} = 1$; note that the average length of the initial chain is 2 which is, correctly, the weight-average.) The programme then evolves the particle by a random walk along the line with appropriate diffusivity, D obeying $D^{-1} \propto L \equiv L_{\text{left}} + L_{\text{right}}$, coupled with random reactions which alter the lengths L_{left} and L_{right} according to whichever reaction scheme is present. The frequency of these processes is governed by the chosen value of the parameter ζ. The time taken for the particles to relax (reach an absorbing end), t_i is recorded and a continuous approximation to the function $\mu(t)$ is constructed as the following sum over N independent trials:

$$\mu(t) = \frac{1}{N} \sum_{i=1}^{N} \theta(t < t_i) \tag{2}$$

With $\theta(t < t_i)$ defined as

$$\theta(t < t_i) = \begin{cases} 1 & \text{if } t_i < t \\ 0 & \text{otherwise} \end{cases} \tag{3}$$

The quantity τ, the stress relaxation time, is also calculated according to,

$$\tau = \int_0^\infty \mu(t)\, \mathrm{d}t \tag{4}$$

Typical N values of 10,000 were found to be necessary to get adequate accuracy at short times. As usual the statistical error decays only as $N^{-1/2}$ and so to maintain a reasonable level of efficiency, the time discretisation step length, δt, was optimized separately for each value of ζ.

It is known that in a time δt a chain may be expected to diffuse a curvilinear distance Δ given by [21], $\Delta = \sqrt{2\, D_c(L)\, \delta t}$, where $D_c(L) = D_o/L$ and D_o is a constant. Each chain has to diffuse, on average, a curvilinear distance $\bar{L}$ to disengage completely from its tube. This process occurs (in the absence of chain reactions) after a time of order τ_{rep}, defined as,

$$\tau_{\text{rep}} = \bar{L}^3/D_o = D_o^{-1} \tag{5}$$

Hence we can rewrite Δ as,

$$\Delta = \sqrt{(2/L)\, \delta \tilde{t}} \tag{6}$$

with $\delta \tilde{t} = \delta t/\tau_{\text{rep}}$. It is known [21] that the disengagement time (longest relaxation time) for an unbreakable chain of length L, τ_d, is given by $\tau_d = L^2/\pi^2 D_c(L)$. Hence we can use this relationship to calculate τ *in the absence of reactions.* Since τ is an average over chain segments (monomers) we have $\tau/\tau_{\text{rep}} = 24/\pi^2 \approx 2.432$. This asymptotic value for τ will appear in the limit of unbreakable chains, $\zeta \to \infty$ (see Fig. 6 below).

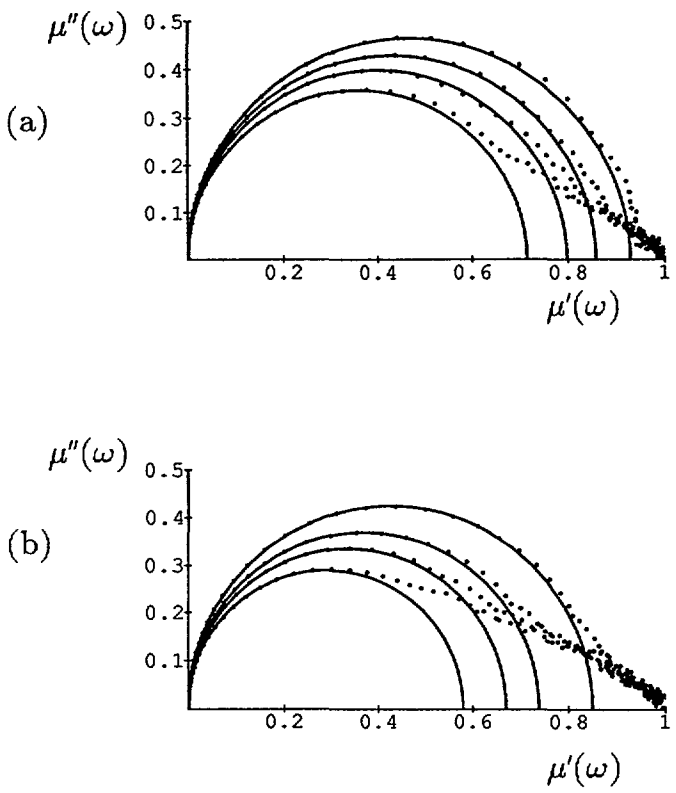

Fig. 4. — (a) Numerically obtained Cole-Cole plots, plotted as $\mu''(\omega)$ vertical and $\mu'(\omega)$ horizontal (with fitted semicircles), for the case when only end-interchange reactions are present. (These results were obtained *without* the treatment of tube renewal detailed in Sect. 4). The plots represent systems with four different values of ζ and $\overline{\zeta}$, from outside to inside, $\zeta = 0.003$, $\overline{\zeta} = 0.133$; $\zeta = 0.03$, $\overline{\zeta} = 0.395$; $\zeta = 0.1$, $\overline{\zeta} = 0.730$; $\zeta = 0.3$, $\overline{\zeta} = 1.308$. (b) Numerically obtained Cole-Cole plots, plotted as $\mu''(\omega)$ vertical and $\mu'(\omega)$ horizontal (with fitted semicircles), for the case when only bond-interchange reactions are present. (These results were obtained *without* the treatment of tube renewal detailed in Sect. 4). The plots represent systems with four different values of ζ and $\overline{\zeta}$, from outside to inside, $\zeta = 0.003$, $\overline{\zeta} = 0.034$; $\zeta = 0.03$, $\overline{\zeta} = 0.142$; $\zeta = 0.1$, $\overline{\zeta} = 0.306$; $\zeta = 0.3$, $\overline{\zeta} = 0.631$.

As mentioned previously, departures from single exponential relaxation are most easily analysed in the frequency domain; hence we define [24],

$$\mu^*(\omega) = \mu'(\omega) + i\,\mu''(\omega) = \frac{G^*(\omega)}{G_o} = i\omega \int_0^\infty e^{-i\omega t}\,\mu(t)\,dt \tag{7}$$

The advantages of studying a frequency dependent modulus $G^*(\omega)$ on a Cole-Cole diagram (one in which $G'(\omega)$ is plotted against $G''(\omega)$) are twofold. Firstly the plot reveals any departure from purely exponential relaxation. This is because exponential relaxation, i.e. $\mu(t) = e^{-t/\tau}$, appears on a Cole-Cole plot as a semicircle passing through $\mu^*(\omega) = 0$ and $\mu^*(\omega) = 1$ and small departures from this exponential form can be easily recognised (see Fig. 4). Conversely when comparing two separate plots of $G'(\omega)$ and $G''(\omega)$ it is not always immediately obvious

when small departures from the exponential form are present. Secondly one can easily identify both the short time scale (high ω) behaviour and the long time scale (low ω) behaviour which are reflected in the form of the plot near $\mu^*(\omega) = 1$ and $\mu^*(\omega) = 0$ respectively, as discussed elsewhere [19].

3.2 REVERSIBLE SCISSION REACTIONS. — In this section we consider the effect of reversible scission reactions, as defined in section 2. This case was studied in detail in reference [19] but the procedure is recalled here for completeness. We define $\zeta = \tau_{\text{break}}/\tau_{\text{rep}}$ where τ_{break} is the expected time for one break to occur on an average chain ($\tau_{\text{break}} = 1/k_s = 2/k'_s$). It should be noted that τ_{rep} is not amenable to separate experimental measurement in living polymer systems. Therefore a knowledge of how the shape of $\mu^*(\omega)$ depends on ζ cannot in itself provide quantitative predictions of the chemical reaction time τ_{break}. For experimental comparison it is appropriate instead to introduce a new quantity $\bar{\zeta}$, defined as $\bar{\zeta} = \tau_{\text{break}}/\tau$ where τ is the stress relaxation time for the system defined in (4). This readily measured quantity is predicted to vary as $\tau \sim \tau_{\text{rep}}\zeta^{1/2}$ for small ζ (in which case, $\bar{\zeta} \simeq \zeta^{1/2}$) but in the crossover region studied here its behaviour is more complicated.

For each ζ value studied the corresponding value of $\bar{\zeta}$ was recorded. The function $\mu(t)$ obtained was then transformed numerically to give predictions for $\mu'(\omega)$ and $\mu''(\omega)$. These are, of course, the storage and loss moduli in units where the plateau modulus is unity.

The probability of a break occuring somewhere on L_{left} (with a similar formula for L_{right}) in time δt (one time step of the algorithm) is p_1, given by,

$$p_1 = L_{\text{left}}\, \zeta^{-1}\, \delta\tilde{t} \tag{8}$$

Should a break occur it does so at a randomly chosen point on L_{left}, equivalent to the transformation $L_{\text{left}} \rightarrow L_{\text{left}} \cdot \phi$ with ϕ uniformly distributed on $[0, 1]$. Similarly we can define the probability of an end-to-end recombination reaction occuring at one end (half the probability of it occuring at either end) in time δt as p_2, given by,

$$p_2 = \zeta^{-1}\, \delta\tilde{t} \tag{9}$$

The result of a recombination reaction on L_{left} (say) is the addition of a length of tube, randomly chosen from an exponential distribution with mean 1, to the end of the chain. This we can write as the transformation $L_{\text{left}} \rightarrow L_{\text{left}} - \ln(\phi)$.

3.3 END-INTERCHANGE REACTIONS. — We now consider end-interchange reactions, as defined in section 2. Any given chain can undergo an end-interchange reaction in one of two ways depending on whether or not the chains own end is involved. If the end of some other chain bites into our test chain somewhere along its length the reaction is denoted A-type. If it is one of the chain's own ends which bites into a second chain the reaction is denoted B-type. We define the time scale on which B-type reactions occur as τ_{break} ($\tau_{\text{break}} = 2/k_e$). We can retain the definitions of $\zeta = \tau_{\text{break}}/\tau_{\text{rep}}$ and $\bar{\zeta} = \tau_{\text{break}}/\tau$ made above although τ_{break} now has a different interpretation in the context of end-interchange reactions.

The probability of an A-type reaction occuring somewhere on L_{left} (say) in time δt is p_A, where $p_A = 2\, p_1$. The effect of an A-type reaction is, with equal probability, either a simple break somewhere randomly chosen on L_{left} or a "reorganisation". A "reorganisation" replaces a randomly chosen fraction of L_{left} with a length chosen from an exponential distribution with mean 1. In fact this is equivalent to the transformation $L_{\text{left}} \rightarrow (L_{\text{left}} \cdot \phi_1) - \ln(\phi_2)$ with ϕ_1 and ϕ_2 both chosen independently from [0,1]. A reorganisation is identical to a scission

reaction immediately followed by a recombination reaction and can be expected to be relatively inefficient at relaxating stress.

The probability of a B-type reaction occuring at one end in time δt is p_B where $p_B = p_2$; the effect of a B-type reaction is statistically identical to a recombination reaction, in that it results in the transformation $L_{\text{left}} \to L_{\text{left}} - \ln(\phi)$. Note that τ_{break}, defined above as $\tau_{\text{break}} = 2/k_e$, is the timescale on which an *effective scission event* occurs, within the end-interchange reaction scheme. Indeed we can interpret half the A and all the B events respectively as "end catalysed" scission and recombination reactions. The dynamics differs from reversible scission only in the presence of a third process, reorganisation, which occurs on the same time scale (τ_{break}) as the others.

3.4 BOND-INTERCHANGE REACTIONS. — Lastly we consider the case of bond-interchange reactions, as defined in section 2. We now define the timescale on which bond-interchange reactions occur to be $\tau_{\text{break}} = 1/k_b$. As in section 3.2 we can retain the definitions of ζ and $\bar{\zeta}$ although τ_{break} now has a different interpretation. The probability of a bond-interchange reaction occuring on L_{left} (say) in time δt is p_1. The effect of a bond-interchange reaction is a pure reorganisation, where $L_{\text{left}} \to (L_{\text{left}} \cdot \phi_1) - \ln(\phi_2)$ as defined in section 3.2.

Stress relaxation in the presence of bond-interchange reactions: the limit $\tau_{\text{break}} \ll \tau_{\text{rep}}$. — If we now consider the limit $\tau_{\text{break}} \ll \tau_{\text{rep}}$ we can make analytic predictions for the stress relaxation within the bond-interchange reaction scheme [23]. Similar predictions, for the case of reversible scission (which carry over to the case of end-interchange) have already been derived, see reference [15]. For bond-interchange kinetics (as for the other two reaction schemes) we predict monoexponential stress relaxation in this limit since the length of chain on which a monomer resides is forgotten on the time scale τ_{break}. For the cases of reversible scission and end-interchange, in the same limit $\tau_{\text{break}} \ll \tau_{\text{rep}}$, the terminal stress relaxation time is given by $\tau \sim \sqrt{\tau_{\text{break}} \tau_{\text{rep}}}$ (see Ref. [15]) whereas for bond-interchange we find instead,

$$\tau \sim \tau_{\text{break}}^{1/3} \tau_{\text{rep}}^{2/3} \tag{10}$$

We obtain equation (10) by using the same arguments as reference [15]: We assume that the rate limiting step for the relaxation of a tube segment involves waiting for a portion of tube of length less than λ to be formed on one side of the segment, where λ is the distance that the chain end can expect to diffuse before it is lost due to another reaction. This will occur after a time $(\bar{L}/\lambda)\tau_{\text{break}}$, the factor $(\bar{L}/\lambda)$ can be thought of as the proportion of all reactions occuring on the portion of length λ, i.e. those reactions which result in a new portion (of order the average length, $\bar{L}$) being substituted for the piece of length λ. This is what we mean when we say that the chain end is lost (bond-interchange reactions do not occur *at* chain ends). Hence we obtain the following equation for λ,

$$\lambda^2 \simeq D_c(\bar{L})(\bar{L}/\lambda)\tau_{\text{break}} \tag{11}$$

In equation (11) above, and throughout the remainder of this section, we ignore numerical factors of order unity which do not affect the result (10).

We now have an equation defining the distance λ, the next step is to write down the expected waiting time for a portion of tube of length less than λ to appear on one side of an average tube segment. This will occur after a time τ, the characteristic relaxation time for the average tube segment. Two factors must be taken into account in determining τ: First we must wait for a bond-interchange reaction to occur within a distance λ of the tube segment; the waiting time

for this is $\tau_{break}\bar{L}/\lambda$. Second we must wait for one of these reactions to substitute a piece of tube of length less than λ at the reaction site. The probability per reaction of this happening is itself of order $\lambda/\bar{L}$. Hence we can write,

$$\tau \simeq \tau_{break}(\bar{L}/\lambda)^2 \tag{12}$$

Eliminating λ from (11) and (12) and recalling equation (5) (which defines τ_{rep} as the inverse of $D_c(\bar{L})$) we obtain the new result (10).

The numerical results presented in figure 6 below can be used to verify the result (10) in the region $\tau_{break}/\tau_{rep} \ll 1$. The slope of the graph, showing $\ln(\tau/\tau_{rep})$ plotted against $\ln(\tau_{break}/\tau_{rep})$, approaches 1/3 in this region, in agreement with equation (10). It can be shown [23] that when $\tau_{break} \ll \tau_{rep}$ (i.e. even when bond-interchange reactions are frequent) the reptation model, on the basis of which (10) was derived, remains an appropriate description.

It is also interesting to consider the dependence of the terminal time τ on concentration in the bond interchange case [23]. Assuming for simplicity a second order rate constant that does not itself depend on concentration, we may follow the arguments of [16] to derive, within a mean field theory, the result $\tau \sim \phi^{11/6}$ with ϕ the volume fraction. This compares with $\tau \sim \phi^{7/2}$ (pure reptation); $\tau \sim \phi^{3/2}$ (reversible scission); and $\tau \sim \phi^{5/4}$ (end interchange), calculated at the same level of approximation. Bond interchange has the largest exponent of the various reaction schemes since, as discussed above, these reactions are less effective (by one power of $\bar{L}/\lambda$) than the others in promoting stress relaxation.

3.5 SUMMARY OF REACTION PROCESSES. — We see that, in terms of their effect on our test chain, all three reaction schemes can be re-interpreted in terms of scission, recombination and reorganisation processes only, albeit with reaction times and probabilities specific to each scheme. It is therefore clear that any "mixture" of the three reaction schemes can easily be incorporated within our algorithm. However, except in section 3.7 where we discuss the case of multiple reaction schemes, we restrict our attention to the three simple cases when each reaction scheme is present alone.

3.6 RESULTS. — For various values of ζ, $\mu^*(\omega)$ and the corresponding values of $\overline{\zeta}$ are calculated. It is found that values of $\overline{\zeta} \ll 1$ give relaxation close to single exponential, with the corresponding Cole-Cole diagrams having a well defined semi-circular character. This result is independent of which of the three reaction mechanisms is present and, in what follows, where we do not specify a precise reaction scheme our discussion applies to all three. The single exponential character of reversible scission / end-interchange has been discussed previously at length [15,19] however the extension to bond-interchange, as described in section 3.4.1, is a new prediction and is verified in the results described below. The single exponential behaviour can be thought of as a motional narrowing of the spectrum [15-17]; when reactions are fast on the time scale of stress relaxation ($\overline{\zeta} \ll 1$), all tube segments relax at the same rate since the position of a segment, and the length of chain it is on, are forgotten on the time scale of the fast process. At short times ($t \leq \tau_{break}$) a spread of relaxation rates is recovered, and indeed there are always departures to the semicircle at very high frequencies (the right hand edge of the plot). For $\overline{\zeta} \simeq 1$, the region of the diagram near (1,0) becomes markedly less semi-circular, corresponding to a relaxation modes significantly different from single-exponential at short time scales. Figure 4 shows some numerical Cole-Cole diagrams in this regime. In the regime $\overline{\zeta} \gg 1$ we find (as expected) a strongly nonexponential relaxation corresponding to the unmodified reptation of polydisperse chains.

A method already exists [19] for extracting an estimate for $\overline{\zeta}$ from a Cole-Cole plot. As previously discussed, this is an important procedure as it allows τ_{break} to be estimated from

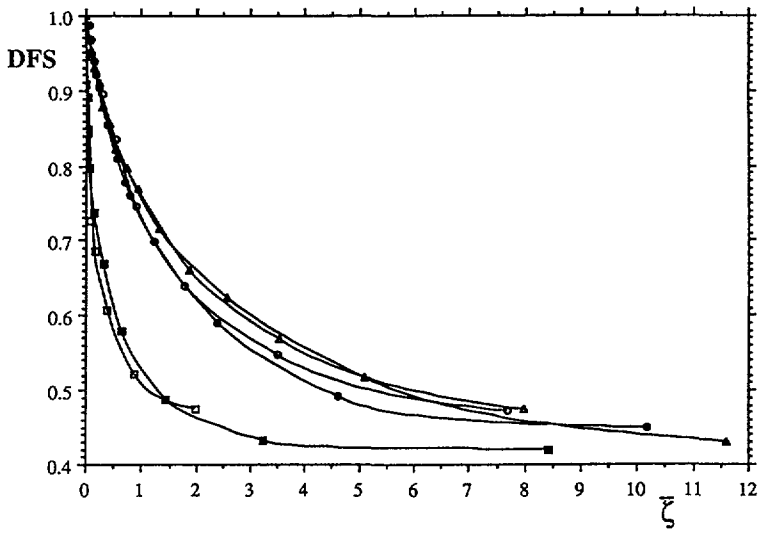

Fig. 5. — Diameter of fitted semicircle (DFS) plotted against $\bar{\zeta}$ (horizontal axis). All three reaction schemes are considered both with and without the treatment of tube renewal effects detailed in section 4. Results for scission/recombination are represented by circles (o), end-interchange by triangles (△) and bond-interchange by squares (□). Hollow symbols ((o) etc.) are results *with* tube renewal and solid symbols ((•) etc.) are results *without* tube renewal. Numerical points joined by simple interpolation and constrained to pass through (0,1).

experimental viscoelastic data. For simplicity we seek to parameterise plots of $G^*(\omega)$ by a single dimensionless number between 0 and 1. The first step is to introduce the rescaling $G^*(\omega) \rightarrow \mu^*(\omega) = G^*(\omega)/G_o$ already assumed above. This can be done either by a direct measurement of the plateau modulus or by another method which we briefly review below (for a full description of this procedure see Ref. [19]). Next we perform a least-squares fit of a semicircle through the portion of the Cole-Cole plot that lies to the left of the maximum of $\mu''(\omega)$. The fit is subject to the constraints that the centre of the semicircle must lie on the $\mu'(\omega)$ axis, and that the semicircle must pass through (0,0). Clearly this procedure is somewhat arbitrary but it has the advantage of simplicity.

We can now extract the diameter of the fitted semicircle (DFS) and use this as our parameter. Having thus defined the DFS, we can compile a plot of our numerically determined values of $\bar{\zeta}$, and the corresponding DFS values for each reaction scheme. For any given experimental Cole-Cole plot one can then extract a DFS value and interpolate the plot to gain quantitative estimate for $\bar{\zeta}$ for each of the three reaction schemes. Since the terminal time τ is readily measured (e.g. from $\mu^*(\omega \rightarrow 0) = i\omega\tau$) this gives an estimate of τ_{break} in each case.

The method for extracting an estimate for G_o, mentioned above, utilises the known form for the stress relaxation at short timescales, $G(t) \sim G_o(1 - t^{1/2})$ (assuming chain motion is still reptation-like at these timescales). Transforming this to frequency space using (7), we find that the asymptotic behaviour of $\mu^*(\omega)$ as $\omega \rightarrow \infty$ produces, on the Cole Cole diagram, a straight line with slope −1 approaching the point $(G_o,0)$. Hence if we have experimental data which is incomplete near the G'-axis we can extrapolate the data using a tangent with slope −1 to find the G' intercept which provides an estimate for G_o.

For each of the three reaction schemes we present, in figure 5, $\bar{\zeta}$ plotted against DFS, and, in figure 6 we plot τ/τ_{rep} against ζ. In both cases a simple interpolation between the points

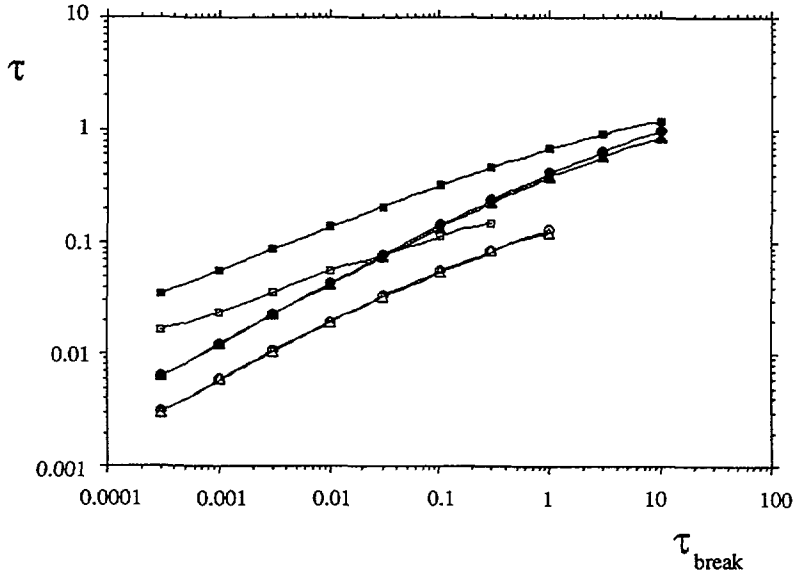

Fig. 6. — The relaxation time τ plotted against τ_{break} (both shown in units of τ_{rep}). All three reaction schemes are considered both with and without the treatment of tube renewal effects detailed in section 4. Results for scission/recombination represented by circles (o), end-interchange by triangles (△) and bond-interchange by squares (□). Hollow symbols ((o) etc.) are results *with* tube renewal and solid symbols ((•) etc.) are results *without* tube renewal. The numerical points joined by simple interpolation.

is included. The errors involved are of the order of a few %. We discuss here only the results obtained without a treatment of tube renewal effects (which are also shown and will be detailed in Sect. 4).

We can see from figure 5 that when bond-interchange reactions *only* are present the DFS value falls more sharply with increasing $\overline{\zeta}$ compared to when either of the other two schemes is present. This implies that, at a constant value of $\overline{\zeta}$, bond-interchange reactions give less single exponential and more reptation-like relaxation than either of the other two schemes. In comparing end-interchange with reversible scission, we recall that for the same τ_{break} end-interchange is identical to scission but with additional reorganisation events taking place on a comparable timescale. These should lead to an additional narrowing of the spectrum (increased DFS) which is indeed observed, although the effect is not large.

Figure 6 enables us to compare τ, the terminal stress relaxation time, at a given value of τ_{break}, when each of the reaction schemes are present (both quantities are in units of τ_{rep}). We see that bond-interchange reactions, which result in reorganisation events, are as expected much less efficient than end-interchange or scission reactions at relaxing stress. End-interchange and scission/recombination reactions show similar relaxation times. This is as expected since end-interchange is statistically equivalent to scission/recombination to within one reorganisation event per τ_{break}. For very large values of τ_{break}, when reactions are rare, the difference between bond-interchange and the other two schemes becomes small. In the opposite limit, for very small values of τ_{break}, the curve for bond-interchange reaches a constant slope of 1/3, and those for reversible scission and end-interchange reach a slope of 1/2. These observations are in agreement with equation (10) and the work of reference [15] respectively.

As discussed elsewhere [19] it is possible to use the relationship between DFS and $\bar{\zeta}$ (as shown diagramatically in Fig. 5), in conjunction with experimental viscoelastic data (yielding values for τ and DFS) in order to determine τ_{break}. Even if it is not known whether scission/recombination or end-interchange reactions are present we can see from figure 5 that the error in interpolating $\bar{\zeta}$ will be less than 10%.

3.7 COMPARISON WITH T-JUMP ESPERIMENTS: MULTIPLE REACTION SCHEMES. — T-jump experiments allow an independent determination of the scission/ recombination breaking time [18] in systems of wormlike micelles although, for reasons of signal strength, this technique is mainly limited to the dilute regime. T-jump experiments measure a relaxation time τ_{tj} which depends only on the reaction rate constant for reversible scission ($\tau_{tj} = 1/2k$) and is quite insensitive to end-interchange reactions [18]. (We disregard bond-interchange reactions for the moment [25]). Hence we can write,

$$\tau_{\text{break (due to scission)}} = 2\,\tau_{tj} \tag{13}$$

If we now assume that reversible scission and end-interchange reactions are approximately equally efficient at stress relaxation (this approximation would be exact if their respective plots in Fig. 5 coincided) then we can, for the first time, consider the case when more than one reaction scheme is present in a given system. For systems in which both reversible scission and end-interchange reactions are present we can write the time scale on which breakage events occur, regardless of their microscopic origin, as $\tilde{\tau}_{\text{break}}$, given by,

$$\frac{1}{\tilde{\tau}_{\text{break}}} \approx \frac{1}{\tau_{\text{break (due to scission)}}} + \frac{1}{\tau_{\text{break (due to end-interchange)}}} \tag{14}$$

where we have had to differentiate between the effects of scission and end-interchange reactions in the same system. It is now $\tilde{\tau}_{\text{break}}$ which is the relevant quantity for stress relaxation and we can re-interpret $\bar{\zeta}$ as $\bar{\zeta} = \tilde{\tau}_{\text{break}}/\tau$. Hence for systems where there exists both viscoelastic and T-jump data it is now possible, in principle, to determine the relative rates of the reaction schemes present by combining (13) and (14). Unfortunately quantitative calculations of this kind require highly accurate experimental data and the required accuracy in $G^*(\omega)$ is probably beyond the reach of contemporary experiments. But even with current experimental techniques we can still hope to identify the dominant reaction scheme present; this is done in the discussion below where we apply the DFS procedure described above to experimental data.

We turn our attention to the system CTAC/NaSal+NaCl [20]. Several sets of viscoelastic experimental data exist for this system [20,26], for various concentrations of each of the components (see, e.g. Fig. 7). However T-jump measurements on these systems [20] are unable to give an accurate value of τ_{tj}, which has so far proved to be too large for experimental measurement; we can only say that $\tau_{tj} \geq 2$ s. We focus on one set of data (that shown in Fig. 7), from which we may obtain an estimate for $\tilde{\tau}_{\text{break}}$, as defined in (14). We can extrapolate the data points to the $G'(\omega)$ axis (using a line with slope −1) in order to obtain an estimate for G_o (we know that the points approach G_o along a line with slope −1 provided reptative relaxation is dominant at all relevant timescales). In this case we extrapolate from the points just to the left of the region of upward curvature and thus ignore the non-reptative behaviour represented in this region. We estimate $G_o \approx 975$ dynes/cm^2, hence DFS≈ 0.77 and, *via* figure 4, $\bar{\zeta} \approx 0.8$. A direct measurement of the viscoelastic time $\tau = 1.148$ s has been made [20]. Hence the viscoelastic data suggests a value for $\tilde{\tau}_{\text{break}} \approx (0.8 \times 1.148) = 0.9$ s. We already know, from $\tau_{tj} \geq 2$ s and equation (13), that $\tau_{\text{break (due to scission)}} \geq 4$ s and so, even allowing

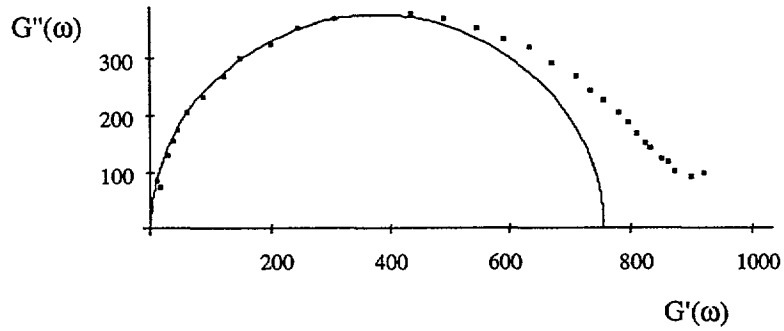

Fig. 7. — Experimental Cole-Cole plot for the system: [CTAC] = 0.15M, [NaSal] = 0.09 M, [NaCl] = 0.1 M, T = 30°C, with τ = 1.148 s. Both axes are in units of dynes/cm^2 and a fitted semicircle is included. The region of upward curvature on the extreme right of the plot (corresponding to very short time scales) may be due to a crossover to the Rouse regime as discussed in reference [19]. Data provided by Kern, Zana and Candau [20,26].

for experimental uncertainty, the breaking of micelles (occuring on a time scale $\tilde{\tau}_{\text{break}}$) must be dominated by some process other than simple scission, in agreement with our predictions for end-interchange. Although our argument, as it stands, cannot rule out the possibilty that bond-interchange reactions dominate, the work of reference [26] provides evidence, based on the volume fraction dependence of the relaxation time τ, that end-interchange reactions do indeed dominate in this system [23].

4. A preliminary treatment of tube renewal effects.

A polymer undergoing diffusive motion in a concentrated solution has its lateral motion restricted by the steric constraints of the neighbouring chains. The entanglements of a chain with its neighbours can be thought of as providing a "tube" along which the chain can undergo curvilinear diffusion. This is the well known tube model [21]. As stated in section 3, where the tube was considered permanent, a small strain distorts distort the tube and the stress associated with this can be relaxed by the reptation of the chain out of its initial tube and into a new tube, which is at equilibrium. However if we consider the tube to be made up of N_e entanglement points each of which is also the tube segment of some other polymer it is apparent that the tube must evolve in time. This concept is not new [27-29] and our model is similar to the "double reptation" model of des Cloizeaux [27]. We assume that each entanglement point disappears when the end of the polymer providing it passes by. Hence each entanglement has a probability $\mu(t)$, as defined in section 3, of still being in existence at a later time t. We now introduce the approximation that the removal of one entanglement point results in the loss of $1/N_e$ of the stress. This approximation does not take into account the fact that new entanglements will appear on roughly the same time scale as the old ones disappear and it also neglects the fact that entanglements consist of more than one chain. However we might expect that some finite number n of these events (where $n \gtrsim 1$) together result in the loss of $1/N_e$ of the stress. In this case our assumption ($n = 1$) provides a lower bound for $\mu(t)$, denoted $\mu_1(t)$. This treatment of constraint release assumes that each tube segment disappears with equal probability due to one of two process, either the disappearance of the test chain or the disappearance of the chain providing the entanglement. This implies that $\mu_1(t)$ is given by

the square of $\mu(t)$, as defined in section 3 (where we neglected tube renewal effects). In the context of our numerical study $\mu_1(t)$ is constructed as follows,

$$\mu_1(t) = \frac{1}{N^2}\left[\sum_{i=1}^{N}\theta(t < t_i)\right]^2 \tag{15}$$

In the limit of exponential relaxation the time τ_n (the relaxation time at a given n) is related to the time τ (the relaxation time in the absence of tube renewal) by,

$$\tau_n = \frac{n\,\tau}{(1+n)} \tag{16}$$

Using our model it is possible to calculate the relaxation function for any $n > 1$ although here we only consider the case $n = 1$, the results for which are included in figures 5 and 6. We can see from figure 5 that our crude treatment of tube renewal effects has a relatively small effect on the variation of $\overline{\zeta}$ with DFS. Since this treatment is expected to overestimate the effect due to tube renewal we can conclude that, at a given value of $\overline{\zeta}$, tube renewal does not alter the DFS value by more than 10% or so. This is an important result since, for many purposes, it allows us to neglect tube renewal effects. For example when interpolating a value for $\overline{\zeta}$, given DFS, a 10% error in the interpolation is probably acceptable. This is reassuring in view of the work of section 3.7 and reference [19], in which a quantitative comparison of breaking times (determined by interpolation from viscoelastic data, and from temperature jump) was made without taking account of tube renewal.

Figure 6 shows that tube renewal effects depress τ, even at large τ_{break} when the relaxation is non exponential (Eq. (16) only holds for exponential relaxation). In order to see how efficient tube renewal might be at releasing stress we see that, even for $\tau_{\text{break}}/\tau_{\text{rep}} < 0.1$, bond-interchange reactions combined with tube renewal result in a lower τ than for either of the other two schemes in the absence of tube renewal. Since we already know that bond-interchange is relatively inefficient at relaxing stress we can attribute this rapid relaxation to tube renewal, although again we emphasise that this represents an upper estimate for the effect of tube renewal on stress relaxation.

5. Conclusions.

Using the model of references [15-17], we have studied in detail for the first time the effect of end-interchange and bond-interchange reactions on the evolution of the linear viscoelastic spectra of living polymers under variation of the ratio $\zeta = \tau_{\text{break}}/\tau_{\text{rep}}$. The effect of scission and end-to-end recombination reactions were also considered, as was the effect of constraint release leading to tube renewal. For suitable definitions of τ_{break} we find that end-interchange can be thought of as equivalent to scission/recombination (at the same value of τ_{break}) to within one, relatively unimportant, "reorganisation" reaction per τ_{break}. We also find that bond-interchange provides only "reorganisation" events and is therefore less efficient at relaxing stress, with a terminal time obeying $\tau \sim \tau_{\text{break}}^{1/3}\tau_{\text{rep}}^{2/3}$ at small ζ. (This result assumes that the identity of the tube is preserved even though bond interchange enables chains to pass through one another at a finite rate [23].)

In all cases, stress relaxation is exponential for $\zeta \ll 1$ and strongly nonexponential for $\zeta \gg 1$. The subtle departures from exponential behaviour in the crossover region are most easily seen in the Cole-Cole representation. We have use a convenient method for parameterising Cole-Cole

plots that are close to semicircular, and shown how this allows the key time scale for reactions, τ_{break}, to be estimated quantitatively from the linear viscoelastic spectra provided the reaction scheme is known. In fact even when it is not known whether scission/recombination or end-interchange reactions dominate or whether tube renewal effects are important it is possible to estimate τ_{break} to within an error of order 20%. Our analysis is only appropriate when reptation is the dominant mechanism of chain motion on the time scale of τ_{break}.

Acknowledgements.

We are grateful to Prof. S. J. Candau for suggesting the usefulness of the Cole-Cole representation and for numerous helpful comments. We wish to thank F. Kern, D. Collin and S. J. Candau for providing the data used in figure 7 and C.Marques and F.Lequeux for discussions regarding equations (10). One of us (M.S.T.) acknowledges the support of S.E.R.C. and the Food Research Institute (Norwich) in the form of a CASE studentship. This work was funded in part by under EC Grant SC1 0288-C.

References

[1] Lang J., Zana R., Chemical Relaxation Methods In Surfactant Solutions, R. Zana Ed. (Marcel Dekker: New York, 1987) p. 405 and references therein.
[2] Kern F., Collin D., Candau S. J., to be published.
[3] Shikata T., Hirata H., Kotaka T., *Langmuir* **3** (1987) 1081.
[4] Shikata T., Hirata H., Kotaka T., *Langmuir* **4** (1988) 354.
[5] Rehage H., Hoffmann H., *J. Phys. Chem.* **92** (1988) 4712.
[6] Hoffmann H., Loebl H., Rehage H., Wunderlich I., *Tenside Deterg.* **22** (1985) 290.
[7] Wunderlich I., Hoffmann H., Rehage H., *Rheol. Acta* **26** (1987) 532.
[8] Porte G., Appell J., *J. Phys. Chem.* **85** (1981) 2511.
[9] Appell J., Porte G., Poggi Y., *J. Colloid Interface Sci.* **87** (1981) 492.
[10] Porte G., Marignan J., Bassereau P., May R., *J. Phys. France* **49** (1988) 511.
[11] Candau S. J., Hirsch E., Zana R., *J. Phys. France* **45** (1984) 1263.
[12] Candau S. J., Hirsch E., Zana R., *J. Colloid Interface Sci.* **105** (1985) 521; *J. Phys. France* **45** (1984) 1263; Physics of Complex and Supermolecular Fluids, S. Safran and N. Clark Eds. (() Wiley, New York, 1987).
[13] Candau S. J., Merikhi F., Watson G., Lemarechal P., *J. Phys. France* **51** (1990) 977.
[14] Cates M. E., Candau S. J., *J. Phys. Condensed Matter* **2** (1990) 6869.
[15] Cates M. E., *Macromolecules* **20** (1987) 2289.
[16] Cates M. E., *J. Phys. France* **49** (1988) 1593.
[17] Cates M. E., *J. Phys. Chem.* **94** (1990) 371.
[18] Turner M. S., Cates M. E., *J. Phys. France* **51** (1990) 307.
[19] Turner M. S., Cates M. E., *Langmuir* **7** (1991) 1590.
[20] Candau S. J., private communication.
[21] Doi M., Edwards S. F., The Theory of Polymer Dynamics (Clarendon, Oxford, 1986) .
[22] de Gennes P. G., Scaling concepts in Polymer Physics (Cornell University Press, Ithica N.Y., 1979) .
[23] Turner M. S., Marques C. M., Cates M. E., in preparation.
[24] Ferry J. D., Viscoelastic properties of polymers (Wiley, N.Y., 1980) .

[25] It is expected that the time τ_{tj} is also insensitive to the presence of bond-interchange reactions. Future work [23] will focus on determining the T-jump relaxation for systems in which bond-interchange kinetics dominate. In any case since equation (18) cannot be directly extended to incorporate bond-interchange reactions (they cannot be described in terms of an "effective scission / recombination rate") we are not able to include them in the following analysis.

[26] Kern F., Zana R., Candau S. J., *Langmuir* **7** (1991) 1344.

[27] Viovy J. L., Monnerie L., Tassin J. F., *J. Polym. Sci. Phys. Ed.* **21** (1983) 2427;
Viovy J. L., *J. Polym. Sci. Phys. Ed.* **23** (1985) 2423.

[28] Marucci G. J., *Polm. Sci., Polym. Phys. Ed.* **23** (1985) 159.

[29] Des Cloizeaux J., *Europhys. Lett.* **5** (1988) 437.